FULL PAPER

Dalton
www.rsc.org/dalton

Molecular design of a proton-induced molecular switch based on rod-shaped Ru dinuclear complexes with bis-tridentate 2,6-bis(benzimidazol-2-yl)pyridine derivatives †

Masa-aki Haga,* Tomohiro Takasugi, Akihiro Tomie, Masahide Ishizuya, Tetsuyuki Yamada, M. Delower Hossain and Miyao Inoue

Department of Applied Chemistry, Faculty of Science and Engineering, Chuo University, 1-13-27 Kasuga, Bunkyo-ku, Tokyo 112-8551, Japan.
E-mail: mhaga@apchem.chem.chuo-u.ac.jp

Received 6th January 2003, Accepted 4th February 2003
First published as an Advance Article on the web 23rd April 2003

New dinuclear Ru complexes of bis-tridentate 2,6-bis(benzimidazol-2-yl)pyridine derivatives, $[Ru_2(terpy)_2(H4Ln)]^{4+}$ (terpy = 2,2′:6′,2″-terpyridine, n = 0~2), have been synthesized. The Ru complexes act as tetrabasic acids, in which N–H protons on benzimidazole moieties are responsible for a deprotonation site. Both the absorption spectra and oxidation potentials are strongly dependent on the solution pH, which leads to the basis of a proton-induced molecular switch. The dinuclear Ru complexes bridged by bis-tridentate bis{2,6-bis(benzimidazol-2-yl)pyridine} show a lower Ru(II/III) oxidation potential but almost similar MLCT absorption maxima, compared to the corresponding dinuclear Ru complexes with "back-to-back" bis-2,2′:6′,2″-terpyridine bridging ligands. These results indicate that the bis-tridentate bis{2,6-bis(benzimidazol-2-yl)pyridine} ligand has a stronger σ/π donor property and a weaker π-acceptor property than the bis-2,2′:6′,2″-terpyridine bridging ligand. The solubility of Ru complexes in solution is progressively decreased with increasing number of phenyl group in the bridging ligand, and therefore it becomes difficult to study the change of chemical properties for external stimuli such as pH change. Immobilization of complexes on a solid surface is one of the approaches to overcome their low solubility. The $[Ru_2(bpbbip)_2$-$(H4L0)]^{4+}$ complex with phosphonate groups (bpbbip = 2,6-bis(1-(4-diphosphonyl)butylbenzimidazol-2-yl)pyridine) was successfully immobilized on an ITO electrode and characterized by means of XPS, and cyclic voltammetry. The Ru complex monolayers exhibit a reversible Ru(II/III) oxidation at +0.80 V *vs.* Ag/AgCl in 0.1 M aqueous $HClO_4$. The immobilized Ru complex monolayer is stable over the pH range 1 < pH < 10. The oxidation potential, $E_{1/2}$, *vs.* pH plot reveals several lines, indicating that the proton-coupled oxidative reactions occur on the ITO surface. The phosphonate-immobilized Ru dinuclear complex monolayers exhibited a stable electrochromic response on an ITO electrode.

Introduction

Dinuclear Ru complexes with a bridging ligand have received much attention in recent years in connection with the design of molecular electronic devices such as molecular wires.[1,2] Electron transfer in dinuclear complexes strongly depends on the nature of the bridging ligand, which can control the strength of electronic coupling and the distance of charge transfer.[3–13] Therefore, the design of the bridging ligand is one of the key issues in realizing molecular electronic devices. Various bis-tridentate ligands based on pyridine groups such as bis-2,2′:6′,2″-terpyridine have been synthesized for connection between two redox centers. Generally speaking, pyridine-containing ligands have relatively low-lying π*-orbitals, and therefore they act as a good acceptor. In contrast, the benzimidazole-containing ligands are poorer π-acceptors and better π-donors. Furthermore, benzimidazole possesses a dissociative imino N–H proton, which can perturb the electronic properties of metal complexes through metal–ligand interaction.[14] Therefore, protonation/deprotonation from metal complexes with benzimidazole derivatives can act as an external trigger signal in molecular based switching devices.[15] We have studied proton-induced tuning or switching of chemical properties in the mononuclear $Ru(bimpyH2)_2$ complex[15] and dinuclear and tetranuclear Ru complexes bridged by 2,2′-bis(2-pyridyl)bibenzimidazole.[16,17] Particularly, the metal–metal interaction, calculated from the intervalence charge transfer band, can be switched by the deprotonation of bridging bibenzimidazole ligand in dinuclear Ru complexes.[15]

The proton is one of the elementary particles bearing high positive surface charge density, and plays an important role in bioenergetic systems such as proton coupled electron transfer reactions and proton pumping through biomembranes. In a photosynthetic membrane, electron flow can be coupled directly to electrolytic flow of protons across the membrane to maintain proton gradients. Thus, the combination of proton transfer and electron transfer is attractive not only in developing biomimetic catalysts but also in designing molecular electronics based on proton movements. Several molecular devices such as fluorescent logic gates and molecular shuttles have been developed on the basis of proton movement as an external stimulus.[18–20] Electronic control of proton transport from the polymer or monolayer films has been reported.[21,22] In the present study, the synthesis of new bis-tridentate bis(benzimidazolyl)pyridine derivatives H4L0–H4L2 (H4 refers to four dissociable protons), which are the analogues of the bis-tridentate back-to-back 2,2′:6′,2″-terpyridine,[23–26] are reported (Scheme 1).

A characteristic of the ligands H4L0–H4L2 is that electronic states in the bridging ligand can be controlled by deprotonation of N–H sites on H4L0–H4L2. We have examined the effect of protonation/deprotonation on spectroscopic and

† Based on the presentation given at Dalton Discussion No. 5, 10–12th April 2003, Noordwijkerhout, The Netherlands.

Electronic supplementary information (ESI) available: observed and calculated isotope patterns of ESI mass spectra for the $[M - 4PF_6 - 2H^+]^{2+}$ ion of $[Ru_2(terpy)_2(H4Ln)]$; ^1H NMR spectrum of $[Ru_2(terpy)_2(H4L1)]$ in $(CD_3)_2SO$; HOMOs and LUMOs for bridging ligands H4L0 and H4L2. See http://www.rsc.org/suppdata/dt/b3/b300130j/

DOI: 10.1039/b300130j

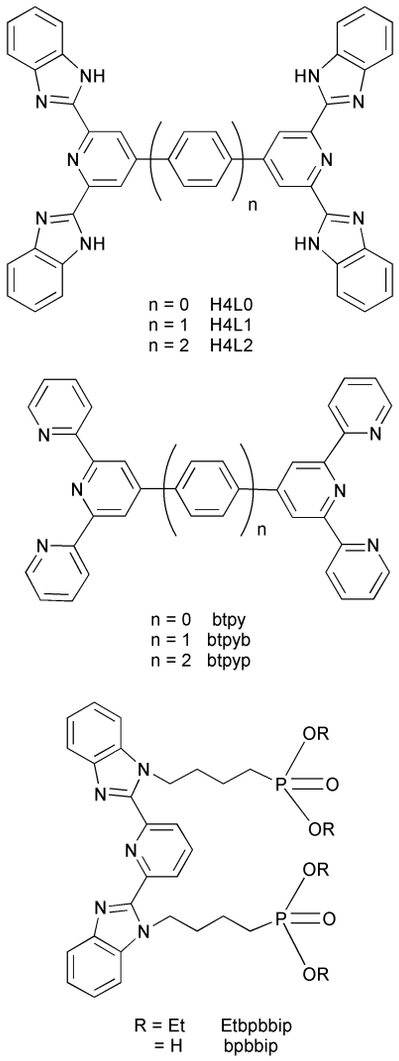

Scheme 1

electrochemical properties in dinuclear Ru complexes with H4L0–H4L2 ligands in solution. We often faced the solubility problem; *i.e.*, precipitation of the Ru complex occurred when the solution pH was changed. For the purpose of overcoming this problem, the surface chemistry of immobilization of the Ru complexes, particularly proton-coupled electron transfer reaction on the surface, was examined by changing the solution pH.

Experimental

Materials

Ruthenium trichloride trihydrate (N.E.Chemcat, Tokyo), 1,4-phenylenediboronic acid (Tokyo Kasei Kogyo (TCI)), 1,4-benzenediboronic acid bis(neopentyl glycol) cyclic ester (Lancaster), $PdCl_2$(dppf) (dppf = 1,1′-bis(diphenylphosphino)-ferrocene) (TCI), $Pd(PPh_3)_4$ (TCI), 1,4-phenyleneboronic acid (TCI), 4-hydroxypyridine-2,6-dicarboxylic acid (TCI), 4,4′-biphenyldiboronic acid bis(neopentyl glycol) cyclic ester (Lancaster), 2,2′,2″-terpyridine (terpy) (Aldrich) were used without further purification. Acetonitrile was purified twice by distillation over P_2O_5. Tetra-*n*-butylammonium tetrafluoroborate ($TBABF_4$, Nacalai) was recrystallized from ethanol–water (4 : 1 v/v) and dried *in vacuo*. All other supplied chemicals were of standard reagent grade quality. The compounds, 2,6-bis(benzimidazol-2-yl)pyridine,[27] 4-bromo-2,6-pyridine dimethyldicarboxylate,[28] $Ru(terpy)Cl_3$, and $[Ru(Etbpbbip)(CH_3CN)Cl_2]$,[29] were synthesized according to literature methods.

Synthesis of ligands

2,6,2′,6′-Tetra(benzimidazol-2-yl)-4,4′-bipyridine (H4L0). This ligand was prepared following the same procedures as used for 2,6,2′,6′-tetra(4,5-dimethylbenzimidazol-2-yl)-4,4′-bipyridine,[30] except 1,2-phenylenediamine was used. The product was soluble in dmf and dmso on heating. Yield: 68%. Mp > 280 °C. ^{1}H NMR (400 MHz, solvent $(CD_3)_2SO$): δ 7.35 (t, J = 7.6 Hz, 4H), 7.38 (t, J = 7.6 Hz, 4H),7.76 (d, J = 7.7 Hz, 4H), 7.86 (d, J = 7.3 Hz, 4H), 8.82 (s, 4H), 13.10 (s, 4H). EI-MS (m/z) = 620 (M^+). Anal. for $C_{38}H_{20}N_{10}\cdot H_2O$. Calc.: C 71.46, H 4.10, N 21.93. Found: C 71.58, H 3.93, N 21.82%.

1,4-Bis(2′,2″,6′,6″-tetracarboxy-1,4′:4,4″-pyridyl)benzene. The complex $PdCl_2$(dppf) (0.0088 g, 0.12 mmol), 4-bromo-2,6-pyridine dimethylcarboxylate (1.08 g, 4.0 mmol), and potassium acetate (1.12 g, 8.0 mmol) were dissolved in degassed dmf (80 cm^3) and stirred for 10 min, and then to the solution 1,4-phenyleneboronic acid (0.37 g, 2.0 mmol) in ethanol (8 cm^3) was added and heated at 90 °C under nitrogen for 48 h by monitoring the complete loss of the starting compound′s spot by TLC (silica gel). After being cooled to room temperature, the solvent was removed *in vacuo*, and the black residue was thoroughly extracted twice with chloroform (200 cm^3). The chloroform extracts were washed with water and brine solution, and then dried over sodium sulfate. The resulting chloroform solution was evaporated *in vacuo* to obtain a brown residue, which was purified by silica gel column chromatography using a mixture of chloroform–ethyl acetate (3 : 1 v/v) as eluent. An analytically pure white powder, the tetramethyl ester, was obtained after removal of solvent. Yield: 42%. Mp > 280 °C. ^{1}H NMR (300 MHz, $CDCl_3$): δ 4.09 (s, 12H), 7.96 (s, 4H), 8.62 (s, 4H). IR(KBr): ν(C=O) 1720 cm^{-1}. ESI-MS (m/z, in CH_3CN–$CHCl_3$ + CH_3CO_2H) = 465.12 (M^+).

Hydrolysis of the isolated tetramethyl ester. The tetramethyl ester (1.01 g, 2.18 mmol) was refluxed in 10% KOH–ethanol (1 : 1 v/v) (300 cm^3) for ~40 h until the TLC spot of the ester disappeared. After cooling, the solution was neutralized with HCl. The resulting white powder was collected by filtration and dried *in vacuo*. The tetracarboxylic acid is sparingly soluble in water and insoluble in common organic solvents. Yield: 84%. IR(KBr): ν(C=O) 1735 cm^{-1}.

1,4-Bis{2,6-bis(benzimidazol-2-yl)pyrid-4-yl}benzene (H4L1). 1,2-Phenylenediamine (0.65 g, 6.0 mmol) was dissolved in polyphosphoric acid (20 cm^3) with stirring at 100 °C under nitrogen, and then 1,4-bis(2′,2″,6′,6″-tetracarboxy-1,4′:4,4″-pyridyl)benzene (0.57 g, 1.39 mmol) was added to the resulting solution. The mixture was heated at 240 °C for 8 h. After this time, the reaction mixture was cooled to room temperature, and poured into water (200 cm^3). The brown precipitate was collected and put into an aqueous solution of 3 M ammonia for neutralization. The resulting precipitate was collected and washed with copious amounts of water, ethanol and ether and dried *in vacuo*. Yield: 0.43 g (46.5%). ^{1}H NMR (400 MHz, solvent $(CD_3)_2SO$): δ 7.32 (t, J = 7.6 Hz, 4H), 7.38 (t, J = 7.6 Hz, 4H), 7.78 (d, J = 7.6 Hz, 4H), 7.84 (d, J = 7.8 Hz, 4H), 8.31 (s, 4H), 8.72 (s, 4H), 13.14 (br, 4H). EI-MS (m/z) = 697 (M^+). M = $C_{44}H_{28}N_{10}$. Anal. for $C_{44}H_{28}N_{10}\cdot 6H_2O$. Calc.: C 65.66, H 5.01, N 17.40. Found: C 65.30, H 4.78, N 16.99%.

4,4′-Bis(2′,2″,6′,6″-tetracarboxy-4,4′:4′,4″-pyridyl)-1,1′-biphenyl. Following the same procedure described above for 1,4-bis(2′,2″,6′,6″-tetracarboxy-1,4′:4,4″-pyridyl)benzene, the reaction of 4-bromo-2,6-pyridine dimethylcarboxylate (2.85 g, 10.4 mmol) with 4,4′-biphenyldiboronic acid bis(neopentyl glycol) cyclic ester (2.0 g, 5.3 mmol) afforded 1.62 g of tetramethyl ester as a white powder. Yield: 56%. IR (KBr) ν(C=O): 1730w cm^{-1}. ^{1}H NMR ($CDCl_3$): δ 4.08 (s, 12H), 7.84 (d, 4H,

J = 8.54 Hz), 7.90 (d, 4H, J = 8.0 Hz), 8.62 (s, 4H). EI-MS (m/z) = 512 (M^+).

Hydrolysis of the isolated tetramethyl ester. The tetramethyl ester (0.89 g, 1.5 mmol) was dissolved in chloroform (100 cm^3), in which potassium hydroxide (5 g) in ethanol (200 cm^3) was added. The solution was refluxed for ~1 h. After the confirmation of complete loss of the starting tetramethyl ester by TLC (~1 h), all the solvents were removed *in vacuo*. The yellow residue was dissolved in water and neutralized with HCl. The resulting pale yellow powder was collected and dried *in vacuo*. Yield: 0.65 g (87%). IR (KBr): ν(C=O) 1725w cm^{-1}.

4,4′-Bis{2,6-bis(benzimidazol-2-yl)pyrid-4-yl}-1,1′-biphenyl (H4L2). The preparation was the same as that of 1,4-bis{2,6-bis(benzimidazol-2-yl)pyrid-4-yl}benzene, except that 4,4′-bis(2′,2″,6′,6″-tetracarboxy-4,4′:4′,4″-pyridyl)-1,1′-biphenyl was used. The ligand is sparingly soluble in common organic solvents. This compound was used without further purification. Yield: 68%. ^{1}H NMR (400 MHz; solvent $(CD_3)_2SO$ + CF_3CO_2D): δ 7.49 (m, 8H), 7.90 (m, 8H), 8.14 (d, 4H, J = 7.8 Hz), 8.23 (d, 4H, J = 7.9 Hz), 8.85 (s, 4H). Anal. for $C_{50}H_{32}N_{10}\cdot 6H_2O$. Calc.: C 68.20, H 5.13, N 15.94. Found: C 67.80, H 4.92, N 15.45%.

Synthesis of anchoring ligand

2,6-Bis(1-(4-diethylphosphonyl)butylbenzimidazol-2-yl)pyridine (Etbpbbip). NaH (oil dispersion 58%); 1.2 g, 50 mmol) was washed with dry n-pentane and then suspended in dried dmf (30 ml). To this suspension was added 2,6-bis(benzimidazol-2-yl)pyridine (3.1 g, 10 mmol) under nitrogen atmosphere and the mixture was heated to 80 °C for 2 h, during which time the suspension slowly dissolved and became a yellow homogeneous solution. The resulting solution, transferred to a dropping funnel using cannula techniques, was added to 1-bromo-4-diethylphosphonylbutane (7.30 g, 27 mmol) in dmf (10 ml) dropwise at room temperature and heated to 100 °C for 10 h. After being cooled to room temperature, a small amount of methanol (1 cm^3) was added and then the solvent was removed under reduced pressure. The resulting residue was dissolved in dichloromethane, purified by column chromatography on silica gel with hexane–ethyl acetate (4 : 1 v/v). The desired compound, eluted as a third band, was obtained as an oil. Yield: 6.65 g (95%). Mass spectrum: m/z = 695.735 $(M + H)^+$. ^{1}H NMR (400 MHz; solvent $(CD_3)_2SO$): δ 1.20 (5, 12H), 1.25 (m, 4H), 1.50 (q, 4H), 1.79 (m, 4H), 3.73 (m, 8H), 4.83 (t, 4H), 7.30 (t, 2H), 7.38 (t, 2H), 7.74 (d, 2H), 7.78 (d, 2H), 8.23 (t, 1H), 8.32 (d, 2H).

Synthesis of dinuclear complexes

$[Ru_2(terpy)_2(H4L1)](PF_6)_4$. The microwave reactor used in the present study, which was purchased from Shikoku Keisoku Ltd., has an integral magnetic stirrer and a fitting for a reflux condenser. The irradiation power of the reactor is 650 W at multimode. The ligand, H4L1 (0.24 g, 0.34 mmol), was dissolved in ethylene glycol (30 ml) by microwave assisted heating at 650 W, and then solid $Ru(terpy)Cl_3$ (0.30 g, 0.68 mmol) was added to the solution. The mixture was intermittently heated by the microwave oven for 10 min. During heating the color of the reaction mixture changed to brown. On cooling to room temperature, water (30 ml) was added to the reaction mixture, followed by filtration. To the filtrate 2 M HCl (0.5 cm^3) and then a saturated solution of NH_4PF_6 were added to complete precipitation. The precipitate was collected and dried *in vacuo*. The purification was performed by SP Sephadex LH-20 column chromatography, using an acetonitrile–methanol mixture (1 : 1 v/v) as eluent. The desired complex was obtained by evaporation of the solvent. Yield: 0.20 g (37%). ^{1}H NMR (400 MHz; solvent $(CD_3)_2SO$): δ 6.00 (d, 4H, J = 8.5 Hz), 7.08 (t, 4H, J = 7.8 Hz), 7.28 (t, 4H, J = 6.3 Hz), 7.35 (t, 4H, J = 7.8 Hz), 7.64 (d, 4H, J = 5.4 Hz), 7.78 (d, 4H, J = 8.1 Hz), 7.96 (t, 4H, J = 8.1 Hz), 8.68 (s, 4H), 8.74 (t, 2H, J = 8.1 Hz), 8.82 (d, 4H, J = 8.1 Hz), 9.23 (d, 4H, J = 8.3 Hz), 9.53 (s, 4H). Anal. for $C_{74}H_{50}N_{16}Ru_2P_4F_{24}\cdot 3H_2O$. Calc.: C 44.45, H 2.82, N 11.21. Found: C 44.74, H 3.43, N 10.93%.

$[Ru_2(terpy)_2(H4L2)](PF_6)_4$. The synthetic procedure was the same as that used for the H4L1 analogue, substituting H4L1 for H4L2. Yield: 75%. ^{1}H NMR (400 MHz; solvent $(CD_3)_2SO$): δ 5.97 (d, 4H, J = 8.5 Hz), 7.07 (t, 4H, J = 8.0 Hz), 7.27 (t, 4H, J = 6.9 Hz), 7.34 (t, 4H, J = 7.7 Hz), 7.62 (d, 4H, J = 5.5 Hz), 7.78 (d, 4H, J = 8.2 Hz), 7.95 (t, 4H, J = 8.5 Hz), 8.41 (d, 4H, J = 8.8 Hz), 8.50 (d, 4H, J = 8.2 Hz), 8.72 (t, 4H, J = 8.0 Hz), 8.81 (d, 4H, J = 7.7 Hz), 9.23 (d, 4H, J = 8.2 Hz), 9.35 (s, 4H). Anal. for $C_{80}H_{54}N_{16}Ru_2P_4F_{24}\cdot H_2O$. Calc.: C 47.12, H 2.77, N 10.99. Found: C 47.54, H 3.02, N 10.63%.

$[Ru_2(bpbbip)(H4L0)](PF_6)_4$. A mixture of $[Ru(Etbpbbip)(CH_3CN)Cl_2]$ (0.54 g, 0.6 mmol) and H4L0 in ethylene glycol was heated for 4 min using a 650 W microwave oven. After cooling to room temperature, water (80 cm^3) and then saturated NH_4PF_6 were added to the solution. The resulting precipitate was collected *in vacuo*. The purification was performed by SP Sephadex LH-20 column chromatography with methanol–CH_3CN (1 : 1 v/v) mixed solvent. Yield: 0.46 g (70%). ^{1}H-NMR (300 MHz, $(CD_3)_2SO$): δ 10.01 (s, 4H), 9.18 (d, J = 7.87 Hz, 4H), 8.99 (s, 4H), 8.82 (t, J = 7.87 Hz, 2H), 7.90 (d, J = 8.4 Hz, 4H), 7.68 (d, J = 7.7 Hz, 4H), 7.40 (t, J = 7.9 Hz, 4H), 7.34 (t, J = 8.0 Hz, 4H), 7.20 (t, J = 7.1 Hz, 4H), 7.12 (t, J = 7.1 Hz, 4H), 6.39 (d, J = 8.4 Hz, 4H), 6.20 (d, J = 8.4 Hz, 4H), 5.08 (br t, 8H), 3.79 (q, J = 7.1 Hz, 16H), 2.02 (br q, 8H), 1.73 (br q, 8H), 1.52 (br t, 8H), 1.02 (td, J = 7.0 and 2.0 Hz, 24H).

Deprotection of ethyl ester groups. Deprotection of ethyl ester groups in the ethylphosphonyl moiety of Etbpbbip was made by the reaction of trimethylsilyl bromide (0.5 cm^3) with $[Ru_2(Etbpbbip)(H4L0)](PF_6)_4$ (0.09 g, 0.041 mmol) in dry acetonitrile at 70 °C for 20 h. After the addition of methanol to the solution, the solvent was evaporated to dryness under reduced pressure. The residue was dissolved in methanol (10 cm^3) and 40 cm^3 of warter was added. After acidification by the addition of HCl, the precipitation was affected by adding saturated NH_4PF_6 to the solution. The precipitate was collected and dried *in vacuo*. Yield: 0.07 g (86%). ^{1}H NMR (400 MHz; solvent $(CD_3)_2SO$): δ 9.99 (s, 4H), 9.16 (d, J = 8.3 Hz, 4H), 8.83 (t, J = 8.0 Hz, 2H), 8.30 (s, 4H), 7.87 (d, J = 8.3 Hz, 4H), 7.68 (d, J = 8.0 Hz, 4H), 7.28 (t, J = 9.0 Hz, 4H), 7.20 (t, J = 8.0 Hz, 4H), 7.14 (t, J = 9.3 Hz, 4H), 7.03 (t, J = 9.0 Hz, 4H), 6.39 (d, J = 8.3 Hz, 4H), 6.22 (d, J = 8.3 Hz, 4H), 5.05 (br t, 8H), 2.00 (br, 8H), 1.67 (br, 8H), 1.24 (br, 8H). Anal. for $C_{92}H_{86}N_{20}O_{12}P_8F_{24}Ru_2\cdot 2H_2O$. Calc.: C 42.41, H 3.48, N 10.75. Found: C 42.18, H 3.82, N 11.16%.

Physical measurements

Electronic absorption spectra were obtained on a Hitachi U-4000 spectrophotometer from 200 to 2500 nm. NMR spectra were measured with a 400 MHz JEOL JNM-GSX 400 or 300 MHz Varian Mercury 300 spectrometer. IR were recorded on a Nicolet FT-IR Magna 560 spectrometer. The mass spectra were measured on a Shimadzu QP1000EX spectrometer for organic ligands and Micromass LCT electrospray mass spectrometer equipped with an electrospray interface (ESI) system for the ligands and Ru complexes. X-Ray photoelectron spectra were measured on a Shimadzu/Krastos Axis HSi X-ray photoelectron spectrometer with monochromated Al-Kα radiation as an excitation source. Binding energies were calibrated using C1s binding energy of 285.0 eV as a reference.

Electrochemical measurements were made at 20 °C with a BAS 100 B/W electrochemical workstation or ALS/CH Model 660A electrochemical analyzer. The working electrode was a BAS glassy-carbon (ϕ 3 mm) or BAS platinum disk electrode

(ϕ 1.6 mm) and the auxiliary electrode was a platinum wire. The reference electrode was $Ag/AgNO_3$ (0.01 M in 0.1 M $TBABF_4$ in CH_3CN), abbreviated as Ag/Ag^+ or Ag/AgCl in aqueous solution. The ferrocenium/ferrocene (Fc^+/Fc in dmf or CH_3CN) oxidation process was used as an internal reference standard and all potentials are reported *vs.* Fc^+/Fc. The $E_{½}$ values for the Fc^+/Fc couple was + 0.09 V *vs.* Ag/Ag^+, which were found to be 0.34 V more negative that that *vs.* SCE. pH measurements were made with a TOA model HM-20E pH meter standardized with buffers of pH 4.01 and 6.89. A 50% dmf–buffer mixture was employed because of the limited solubility of the present complexes in pure aqueous solution. The readings of the pH meter in this mixture are referred to as "apparent" pH unless otherwise stated. Spectrophotometric titrations were performed in an acetonitrile or dmf–buffer (1 : 1 v/v) solution, as described previously.[50] Robinson–Britton buffer was used over the pH range 2.0–10.0. Under the acid–base equilibria, the half-wave potential $E_{½}$ of the present dinuclear Ru complex can be expressed by the following equation:

$$E_{1/2} = E^0_{1/2} + \frac{RT}{2F}\ln\left(\frac{\alpha_{red}}{\alpha_{ox}}\right)$$

$$\alpha_{red} = 1 + \frac{K_{11}}{[H^+]} + \frac{K_{11}K_{12}}{[H^+]^2} + \frac{K_{11}K_{12}K_{13}}{[H^+]^3} + \frac{K_{11}K_{12}K_{13}K_{14}}{[H^+]^4} \quad (1)$$

$$\alpha_{ox} = 1 + \frac{K_{21}}{[H^+]} + \frac{K_{21}K_{22}}{[H^+]^2} + \frac{K_{21}K_{22}K_{23}}{[H^+]^3} + \frac{K_{21}K_{22}K_{23}K_{24}}{[H^+]^4}$$

where $E_{½}$ is the standard redox potential of the Ru(II)–Ru(II)/Ru(III)–Ru(III) couple at pH 0 and K_{mn} (m = 1 or 2; n = 1~4) describes the acid dissociation constants (see Scheme 3). Nonlinear regression analysis of the $E_{½}$ *vs.* pH data was carried out to determine the K_{mn} values.

Spectroelectrochemistry was performed using a platinum minigrid (80 mesh) working electrode in a thin-layer cell (optical path length 0.05 cm). The cell was placed into the spectrophotometer, and the absorption change was monitored during electrolysis. An indium–tin oxide (ITO) electrode, purchased from Central Glass Co. (surface resistance < 10 Ω cm^{-1}), was cleaned by the sonication in a mixture of H_2O–H_2O_2–NH_4OH (5 : 1 : 1 v/v), washed by methanol and then water. This precleaned ITO electrode was then immersed in a 0.01 mM methanol solution of the Ru complexes. Differential absorption spectra were measured on the homemade thin-layer cell, in which the immobilized ITO glass was the working electrode and UV cell window at the same time. The cell length and cell volume are 0.5 mm and 0.22 dm^3.

Results and discussion

Preparation of bridging ligands and complexes

As a tridentate ligand, synthesis of 2,2′:6′,2″-terpyridine derivatives have been extensively carried out over the last two decades.[31–41] Particularly, bis(2,2′:6′,2″-terpyridine) ligands linked by conjugated organic groups have been used as a molecular wire to bridge two metal ions and electron transfer mediation through the ligand studied .[4,8,42–44] On the other hand, reports on the synthesis of bis-tridentate benzimidazole derivatives are rare. Recently, we preliminarily reported the preparation of 2,6,2′,6′-tetra(4,5-dimethylbenzimidazol-2-yl)-4,4′-bipyridine and its Ru dinuclear complexes.[30] In order to extend the bridging ligand system with benzimidazole derivatives, we have succeeded in synthesizing a series of bis(2,6-pyridyl) tetracarboxylic acids linked by polyphenylene groups, which can be easily converted to the benzimidazole derivates by the Phillips condensation reaction in high yield (Scheme 2).

Increasing the number of phenyl groups, solubility of the ligand becomes low as expected. The H4L1 ligand is soluble in polar solvents such as dmf and dmso, while H4L2 ligand is insoluble in all the common solvents at room temperature except dmso under acidic conditions. While the conventional heating was tedious and time-consuming for the reaction of insoluble H4L2 ligand with $Ru(terpy)Cl_3$, the microwave assisted heating in ethylene glycol accelerated the reaction and gave the product in good yield.[45] After complexation of the ligand to Ru ions, the solubility was increased and easily purified and characterized by conventional analytical methods. The isotope patterns of ESI mass spectra for the new Ru dinuclear complexes are provided as ESI (Fig. S1). The observed isotope distribution patterns were reproduced by simulation of the expected chemical formulae for the corresponding dinuclear Ru complexes.

The increase in numbers of phenyl groups on bridging ligands leads to the lowering of solubility of both bridging ligands and their complexes in common organic solvents. Sometimes the precipitation occurred when the solution pH was changed. However, once the ligand or complex is immobilized on the solid surface, there are no such solubility problems. Therefore, we have prepared a novel Ru dinuclear complex with novel anchoring ligand, 2,6-bis(1-(4-phosphonyl)butylbenzimidazol-2-yl)pyridine (bpbbip), $[Ru_2(bpbbip)(H4L1)](PF_6)_4$. A phosphonate group has a strong affinity for a metal oxide surface such as ITO.[46,47] As expected, the Ru complex was successfully immobilized on an ITO surface, which makes it possible to study the proton-coupled electron transfer reaction at the surface.

NMR spectra

The ^1H NMR spectra of the complex, $[Ru_2(terpy)_2(H4L2)]$, exhibit a total of 13 resonances as shown in Fig. 1, which correspond to a symmetrical arrangement around the two Ru coordination environments. The ^1H NMR spectrum of $[Ru_2(terpy)_2(H4L1)]$ is given as a ESI (Fig. S2). H–H COSY spectra readily establishes these resonances as corresponding to two terminal terpy moieties and two 2,6-bis(benzimidazol-2-yl)-pyridine. The central pyridyl or biphenyl protons such as H11 and H12 for $[Ru_2(terpy)_2(H4L1)]$, and H11 for $[Ru_2(terpy)_2(H4L2)]$, of the bridged moiety show no cross peak. Furthermore, the deprotonation of the N–H proton in $[Ru_2(terpy)_2(H4L2)]$ induces an upfield shift for almost all protons. In particular, H8, H9, and H11 show a large upfield shift (~0.6 ppm),

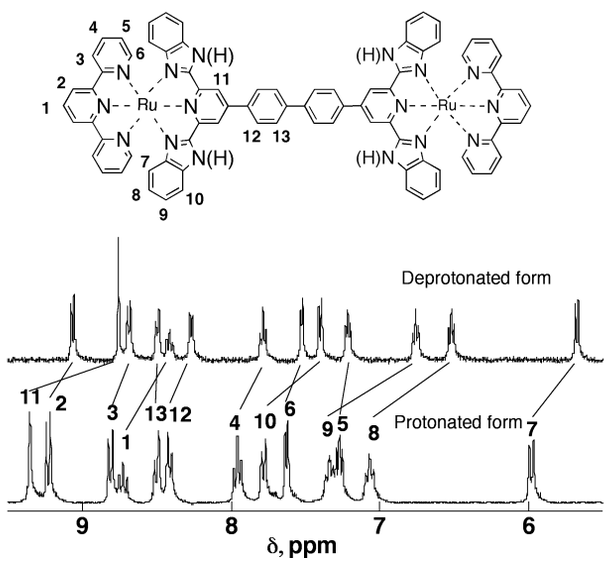

Fig. 1 ^1H NMR spectra of the protonated complex, $[Ru_2(terpy)_2(H4L2)]$ and the deprotonated one, $[Ru_2(terpy)_2(H4L2)]$ in $(CD_3)_2SO$.

Table 1 Spectroscopic and electrochemical data for $[Ru_2(terpy)_2(BL)]$ (BL = H4L0, H4L1 and H4L2) in dmf

		Protonated form		Deprotonated form		
BL	Ru–Ru distance/nm	λ_{max}/nm	ε/dm^3 mol^{-1} cm^{-1}	λ_{max}/nm	ε/dm^3 mol^{-1} cm^{-1}	$E_{½}$/V (ΔE_p/mV)[a]
H4L0	1.15	277	(48000)	275	(102000)	0.69 (70)
		317	(73800)	317	(73400)	
		362	(29200)	345	(58600)	
		510	(29200)	542	(30100)	
H4L1	1.57	274	(39700)	277	(63500)	0.56 (69)
		317	(74200)	317	(58600)	
		356	(49900)	341	(51000)	
		425	(11300)	436	(18900)	
		499	(34900)	530	(23300)	
H4L2	2.00	275	(37900)	275	(46700)	0.54 (70)
		317	(78700)	317	(68700)	
		355	(68400)	342	(66500)	
		417	(15600)	426	(21300)	
		494	(38200)	522	(20600)	

[a] For the protonated form *vs.* Fc/Fc^+.

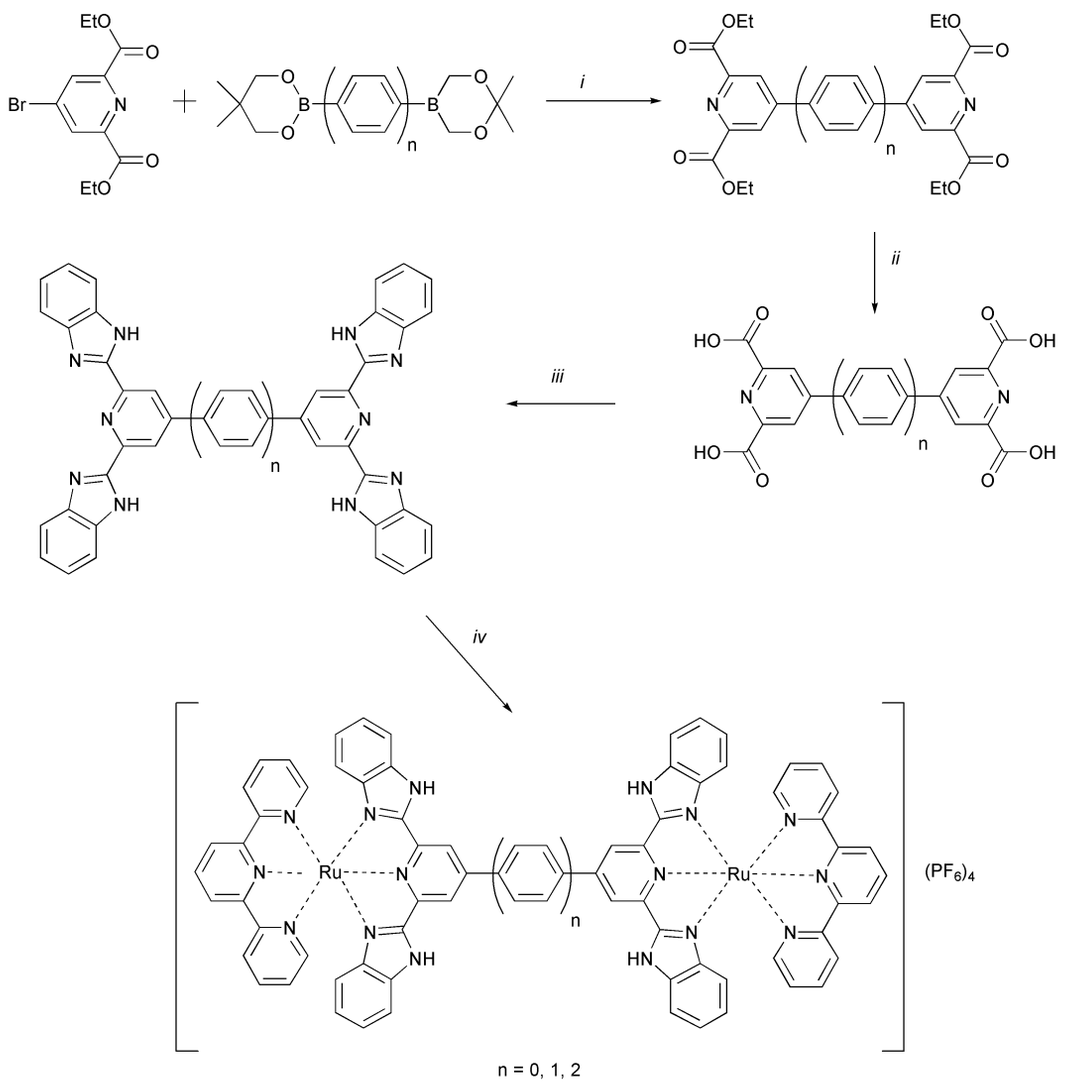

Scheme 2 (i) $PdCl_2$(dppf) and KOAc in dry dmf; (ii) KOH in EtOH–$CHCl_3$; (iii) *o*-phenylenediamine in polyphosphonic acid; (iv) $RuCl_3$(terpy) in ethylene glycol, and NH_4PF_6 in water.

which indicates that the deprotonation leads to the accumulation of electron density on these carbon–H8, –H9, and –H11 moieties. Unfortunately, we could not obtain an NMR spectrum for the deprotonated state of $[Ru_2(terpy)_2(H4L1)]$ because of low solubility in dmso and dmf.

Absorption spectra

The spectral data are summarized in Table 1. The Ru dinuclear complexes exhibit a metal-to-ligand charge transfer (MLCT) band in the wavelength range of 510~495 nm. The MLCT band

maxima are almost the same compared with those of the relevant dinuclear Ru complexes with terpy bridging ligands. In addition, the ligand π–π* transitions of H4L*n* and terpy appeared at 336~355 nm and 317 nm, respectively. By changing the bridging ligand BL in the complexes of $[Ru_2(terpy)_2(BL)]$, the MLCT band energies (BL = bridging ligand) are shifted to a longer wavelength in the order of H4L2 < H4L1 < H4L0. As the number of phenyl spacers in BL is decreased, the MLCT band moves to a longer wavelength. This is due to the increasing interaction of the two bis(benzimidazolyl)pyridine ends of the bridging ligand, which lowers the energy of the bridging ligand π* orbital. A similar trend was observed in the analogous series of $[Ru_2(terpy)_2(L)]$ dinuclear complexes with back-to-back terpyridine bridging ligands such as btpy, btpyb, and btpyp.[6]

The UV spectra of $[Ru_2(terpy)_2(H4Ln)]$ (n = 0 and 2) are very sensitive to solution pH. The pH dependence of the absorption spectra is shown in Fig. 2 for $[Ru_2(terpy)_2(H4L0)]$. From pH

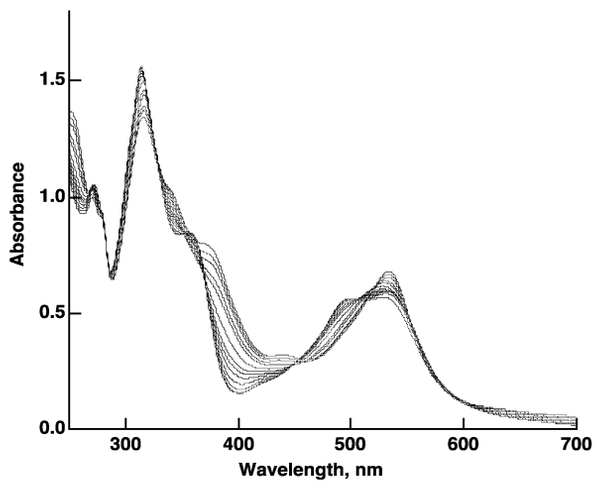

Fig. 2 pH dependence of the absorption spectra for $[Ru_2(terpy)_2(H4L0)]$ in dmf–buffer (1 : 1 v/v) in the region 2.28 < pH < 9.64.

2.25 to 10.53, the absorption maximum at 490 nm decreases and then the two split MLCT bands collapse to a single MLCT band at 533 nm. In addition, a new shoulder at 360 nm for the ligand π–π* transitions of deprotonated L0 appears. Since the $[Ru_2(terpy)_2(H4L0)]^{4+}$ complex has four dissociable NH protons, sequential acid–base equilibria are present as shown in eqn. (2), in which five equilibrium species are present.

$$[Ru_2(terpy)_2(H4L0)]^{4+} \overset{pK_{a1}}{\rightleftharpoons} [Ru_2(terpy)_2(H3L0)]^{3+} \overset{pK_{a2}}{\rightleftharpoons} [Ru_2(terpy)_2(H2L0)]^{2+} \overset{pK_{a3}}{\rightleftharpoons} [Ru_2(terpy)_2(HL0)]^{+} \overset{pK_{a4}}{\rightleftharpoons} [Ru_2(terpy)_2(L0)]^{0} \quad (2)$$

From simulation of the titration curve for the plots of absorbance *vs.* pH, the pK_a values are obtained as pK_{a1} = 4.50, pK_{a2} = 5.70, pK_{a3} = 7.80 and pK_{a4} = 8.90. Fig. 3 shows the pH dependence of UV spectra for $[Ru_2(terpy)_2(H4L2)]^{4+}$ in dmf–buffer (1 : 1 v/v). From this spectral change, we have determined four pK_a values as pK_{a1} = 4.86, pK_{a2} = 5.75, pK_{a3} = 7.00 and pK_{a4} = 8.50. Unfortunately, we could not obtain quantitative spectrophotometric titration data for $[Ru_2(terpy)_2(H4L1)]$ because of its low solubility in CH_3CN–buffer and dmf–buffer, particularly at pH > 5.

Oxidation properties of the Ru complexes in solution

All the Ru complexes, $[Ru_2(terpy)_2(H4Ln)]$ (n = 0, 1, and 2), in dmf in the presence of 10 μl $HClO_4$ show only one reversible Ru(II)/Ru(III) oxidation wave at +0.69 V *vs.* Fc^+/Fc for n = 0, +0.56 V for n = 1, and +0.54 V for n = 2, respectively. Changing

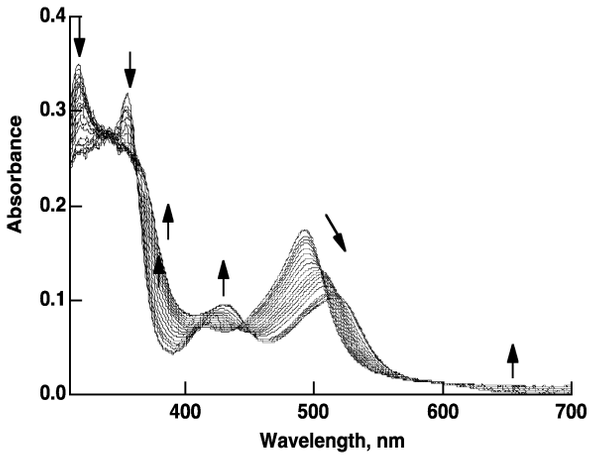

Fig. 3 pH dependence of the UV spectra for $[Ru_2(terpy)_2(H4L2)]^{4+}$ in dmf–buffer (1 : 1 v/v) in the region 3.60 < pH < 10.50.

the bridging ligand in $[Ru_2(terpy)_2(BL)]$, the oxidation potential is shifted to the positive direction in the order of H4L2 ≤ H4L1 < H4L0.

The present Ru complexes with benzimidazole groups have a more negative potential for the Ru(II/III) oxidation process than the analogous $[Ru_2(terpy)_2(BL)]$ complexes (BL = btpy, btpyb, and btpyp).[42,48] This result arises from the stronger donor property of bis(benzimidazolyl)pyridine groups in bridging ligands than that of terpyridine groups.[49,50] The coulometry of the Ru dinuclear complexes indicated that the oxidation process involves two electrons. The presence of only a single oxidation wave suggests that there is little or relatively weak interaction between two Ru centers. Fig. 4 shows the oxidative spectroelectrochemistry of $[Ru_2(terpy)_2(H4L0)]$, at +0.90 V *vs.* Fc^+/Fc in CH_3CN. For the oxidation, the complete disappearance of the Ru(II)-to-ligand MLCT band at 490 and 530 nm and the appearance of a new band near 700 nm originating from a ligand-to-Ru(III) LMCT transition, was observed. Similarly, the oxidative spectroelectrochemistry of other dinuclear Ru complexes has been studied, and showed the disappearance of an MLCT band at around 500 nm and the appearance of an LMCT band at 750 nm.

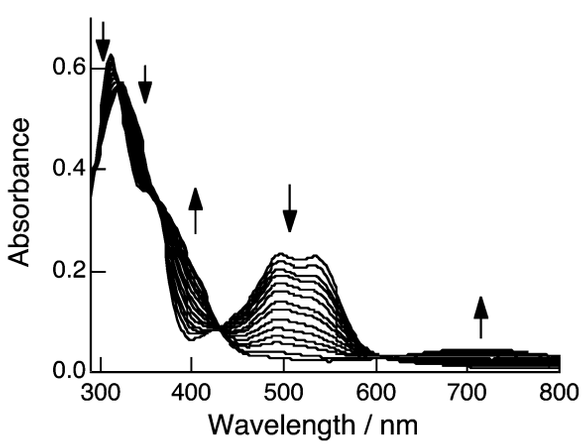

Fig. 4 UV spectral change on oxidative spectroelectrochemistry of $[Ru_2(terpy)_2(H4L0)]$ at +0.90 V *vs.* Fc/Fc^+ in CH_3CN.

The oxidation potentials of the dinuclear $[Ru_2(terpy)_2(H4Ln)]$ complexes in dmf–buffer (1 : 1 v/v) show a strong pH dependence. Fig. 5 shows the half-wave potential, $E_{1/2}$ *vs.* pH diagram for dinuclear $[Ru_2(terpy)_2(H4L0)]$, where the half-wave potential is calculated as the average of the anodic and cathodic peak potentials. The electrode processes for the two-electron Ru(II)-Ru(II)/Ru(III)-Ru(III) couple can be described in terms of Scheme 3. The $E_{1/2}$–pH diagram was analyzed according to the procedure described in the Experimental.

Table 2 Comparison of spectral and electrochemical data

Complex	λ_{max}(MLCT)/nm (ε/dm^3 mol^{-1} cm^{-1})	$E_{½}$ (Ru$^{II/III}$)/V *vs.* Fc/Fc$^+$	Ref.
$[Ru(ttpy)_2]^{2+}$	490 (29000)	0.87	6
$[Ru(terpy)_2]^{2+}$	475 (11000)	0.92	49
$[Ru(bpimH2)_2]^{2+}$	475 (17400)	0.39	50
$[Ru_2(ttpy)_2(btpy)]^{4+}$	520 (58000)	0.93	42
$[Ru_2(terpy)_2(btpy)]^{4+}$	514 (49600)	0.96	26
$[Ru_2(terpy)_2(H4L0)]^{4+}$	510 (29200)	0.69	This work
$[Ru_2(ttpy)_2(btpyb)]^{4+}$	499 (63000)	0.89	42
$[Ru_2(terpy)_2(btpyb)]^{4+}$	492 (44300)	0.93	26
$[Ru_2(terpy)_2(H4L1)]^{4+}$	499 (34900)	0.56	This work
$[Ru_2(ttpy)_2(btpyp)]^{4+}$	495 (58000)	0.88	42
$[Ru_2(terpy)_2(H4L2)]^{4+}$	494 (38200)	0.54	This work

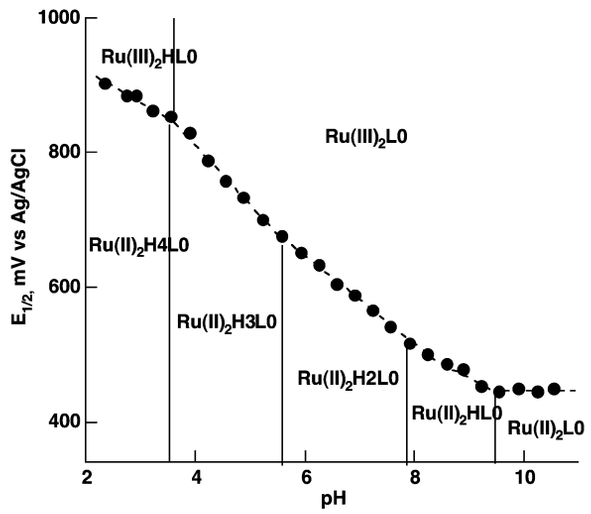

Fig. 5 The half-wave potential, $E_{½}$ *vs.* pH diagram for the dinuclear $[Ru_2(terpy)_2(H4L0)]$ in dmf–buffer (1 : 1 v/v).

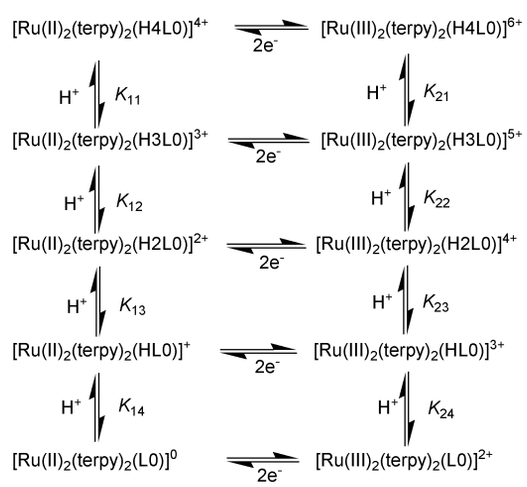

Scheme 3

Over the pH range 2.3–3.8 and 5.8–7.9, the $E_{½}$ value decreases linearly with increasing pH with a slope −55 mV per pH unit, indicative of a two-electron, two-proton process. At 3.8 < pH < 5.8 and 7.9 < pH < 9.3, a plot of $E_{½}$ *vs.* pH is linear with slopes of −90 mV per pH unit and 33 mV per pH unit, consistent with a two-electron, three-proton and a two-electron, one proton processes. Above pH > 9.3, the potentials are pH independent.

For the other Ru dinuclear complexes, the measurements of pH dependent cyclic voltammetry have not been performed because of the low solubility of the complexes.

Characteristics of bridging ligands

The metal–metal interaction in dinuclear Ru complexes can be controlled by a bridging ligand. While many bis-bidentate bridging ligands for dinuclear $Ru(bpy)_2$ complexes have been synthesized, the example of bis-tridentate ligands are still scattered.[51] Mainly the "back-to-back" 2,2′:6′,2″-terpyridine derivatives have been reported. A comparison of MLCT absorption maxima and oxidation potentials for the present Ru dinuclear complexes with those for the corresponding Ru complexes bridged by bis-terpyridine ligand is shown in Table 2. While the MLCT absorption maxima are almost the same for the two complexes, the oxidation potential is 0.2~0.3 V lower for the H4L*n* system than for the bis-terpy system.[49,50] This result is rationalized by the stronger interaction between Ru dπ orbitals and the ligand with σ/π-donor property of benzimidazole groups, which results in the higher HOMO energy. On the other hand, the energy gap between HOMO and LUMO levels is almost unchanged between the bis-terpy bridging Ru dinuclear system and the bis-2,6-bis(benzimidazol-2yl)pyridine bridging one.

In order to examine the feature of the bridging ligand in comparison with terpy bridging ligands, the *ab initio* MO calculation of free ligands, H4L0, H4L1, and H4L2 have been carried out using Spartan™ software.[53] For the calculation, the bis(benzimidazolyl)pyridine moieties are frozen as a coplanar structure. As expected, the biphenyl-type twisting between two bis(benzimidazolyl)pyridine moieties is present for the optimized geometries. The dihedral angle between two bis(benzimidazolyl)pyridine moieties in the ligand H4L0 is 77.8°, which is close to an orthogonal orientation. For the optimized geometries, the two dihedral angles of the bis(benzimidazolyl)-pyridine–phenyl plane are 38.3 and 39.0° for H4L1, and 38.5 and 37.2° (central phenyl–phenyl groups) for H4L2. The HOMO and LUMO energies become higher in the order H4L0 < H4L1 < H4L2 and H4L1 < H4L2 < H4L0, respectively. The common characteristic of the bridging ligands for H4L0, H4L1, and H4L2 is that the electron densities in the HOMO are mainly localized on benzimidazole moieties and those in the LUMO are localized on central bridged phenylene–pyridine moieties (see Fig. S3, ESI). Therefore, the pathway for metal–metal interaction occurs through Ru(II)dπ–bridging ligand LUMO interaction. The MO calculation reveals that deprotonation from the bridging ligand H4L*n* induces a rise in all the orbital energies. The HOMO and LUMO energies of fully deprotonated ligands become higher in the order L2 < L1 < L0 and L2 < L1 < L0, respectively. The Ru(III)dπ–ligand HOMO interaction plays an important role after deprotonation. In addition, deprotonation induces a conformational change in the dihedral angle between two bis(benzimidazolyl)pyridine C–C bonds in H4L0 from ~78 to ~40°. The energies of H4L1 and H4L2 are strongly dependent on the aryl-ring conformation.

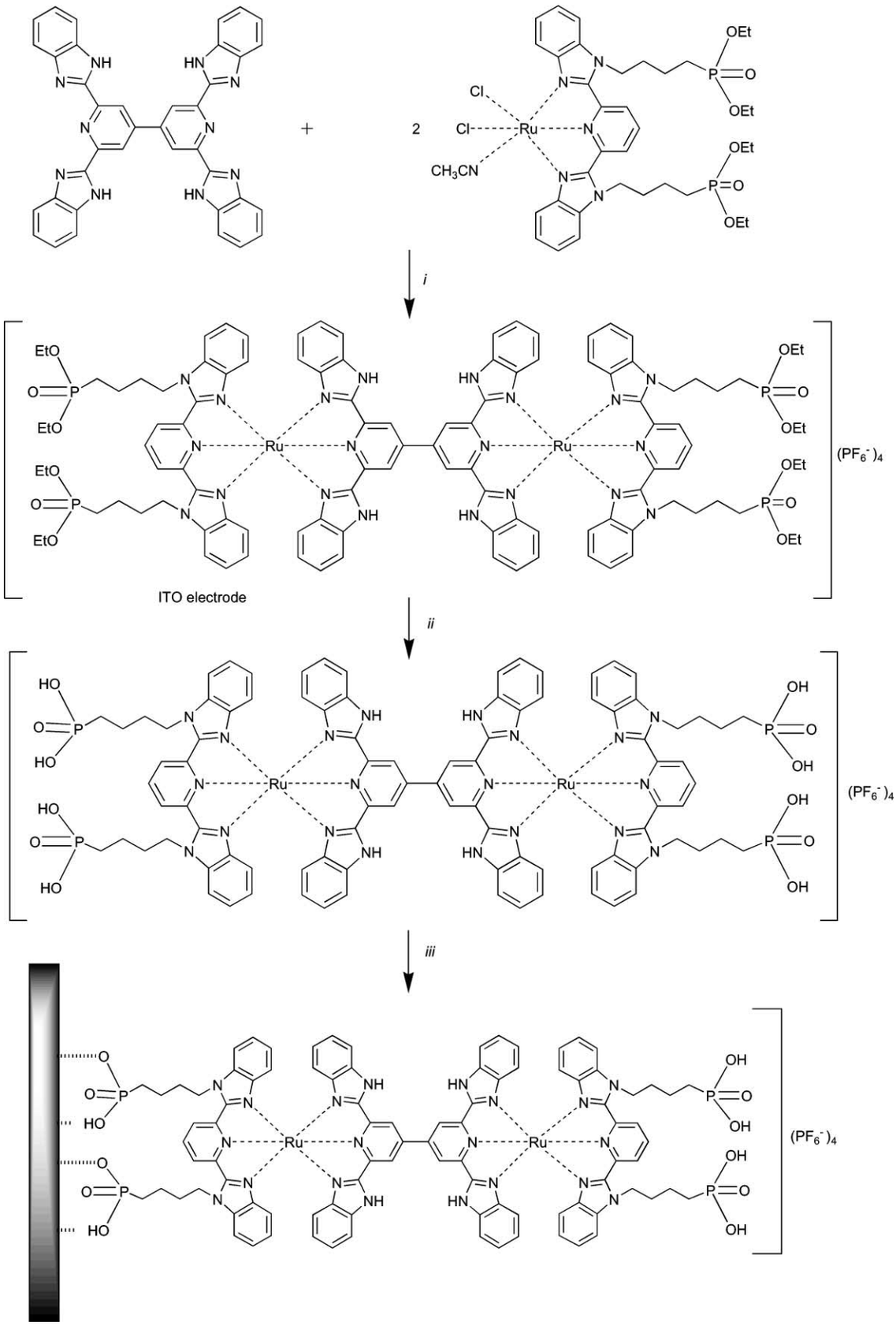

Scheme 4 (i) In ethylene glycol/microwave assisted heating, and NH_4PF_6 in water; (ii) Me_3SiBr in dry CH_3CN and the addition of CH_3OH, then NH_4PF_6 in water; (iii) immersion of ITO electrode in a methanol solution of the complex.

Immobilization of dinuclear Ru complexes on an ITO electrode

As the number of phenyl groups in the bridging ligand is increased, the solubility of the Ru dinuclear complexes becomes lower. Therefore, study in solution becomes difficult. However, this difficulty can be partially solved when the complex is immobilized on a surface. In the present study, phosphonate groups were used as an anchoring group to a metal oxide surface since self-assembly of phosphonate on metal oxide surfaces has been reported previously.[46,52] The synthetic scheme for new dinuclear Ru complexes with anchoring phosphonate groups is shown in Scheme 4. The surface immobilization of

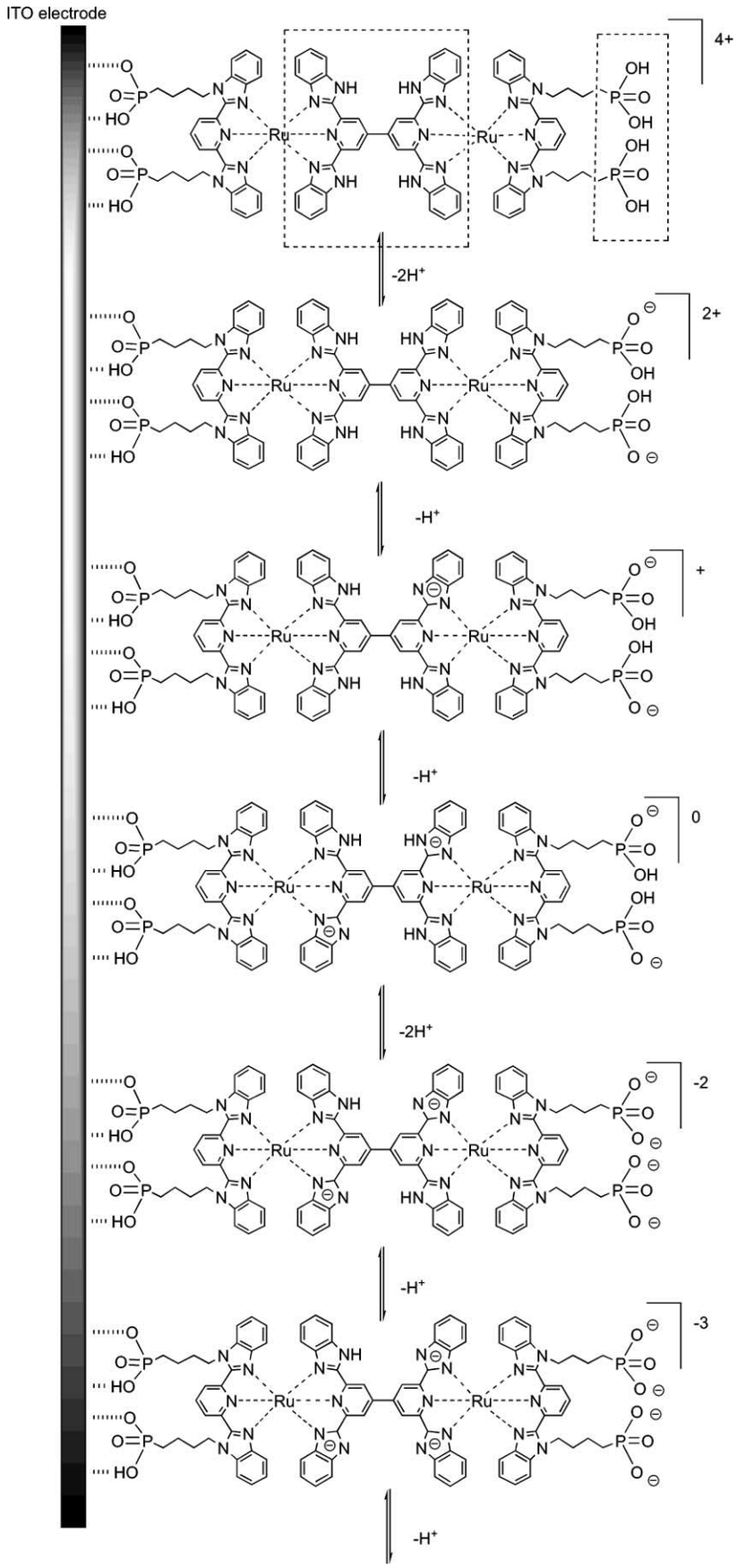

Scheme 5 Proton transfer equilibria of $[Ru_2(bpbbip)_2(H4L0)]^{n+}$ on an ITO surface.

Ru complex, $[Ru_2(bpbbip)_2(H4L0)](PF_6)_4$, was performed by the immersion of ITO substrates directly into an acetonitrile–methanol solution of $[Ru_2(bpbbip)_2(H4L0)](PF_6)_4$. The adsorption process of $[Ru_2(bpbbip)_2(H4L0)](PF_6)_4$ on an ITO electrode was monitored by UV spectroscopy. Increases in absorbance at 330 nm correspond to the π–π* transition and the band at 540 nm is assigned to a MLCT transition. The time profile of the adsorption follows the diffusion-controlled adsorption under a linearized isotherm. The XPS spectrum of the ITO surface gave characteristic C 1s, Ru 3d, N ls, O 1s and P 2p

peaks in addition to the Sn 3d, and In 3d peaks from the ITO substrate, which strongly indicates the immobilization of $[Ru_2(bpbbip)_2(H4L0)](PF_6)_4$ on the ITO surface.

Proton-coupled electron transfer at an ITO solid surface

Cyclic voltammetry of $[Ru_2(bpbbip)_2(H4L0)](PF_6)_4$ immobilized on an ITO electrode in 0.1 M $HClO_4$ exhibits the Ru(II/III) oxidation process at 0.79 V *vs.* Ag/AgCl, which strongly depends on the solution pH. The surface coverage is $(0.80 \pm 0.04) \times 10^{-10}$ mol cm^{-2}. The immobilized Ru complex on an ITO electrode is stable over the range $1 < pH < 10$. The pH dependent cyclic voltammograms in acetonitrile–Britton–Robinson buffer (1 : 1 v/v) are shown in Fig. 6.

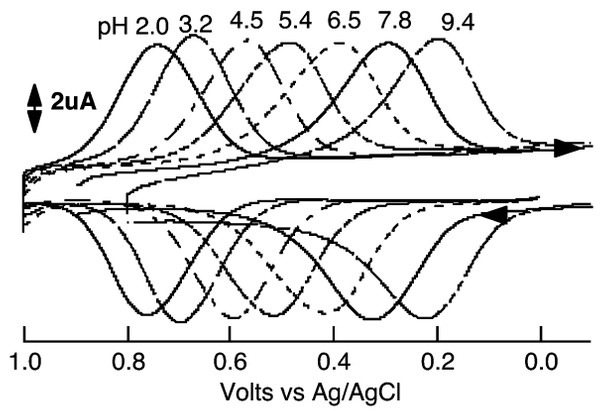

Fig. 6 pH dependent cyclic voltammograms of $[Ru_2(bpbbip)_2(H4L0)](PF_6)_4$ in CH_3CN–Britton–Robinson buffer (1 : 1 v/v) at various pHs.

The oxidation potential *vs.* pH plots reveal several lines. Over the ranges of pH 1–3.5, 3.5–6.0, 6.0–8.0, and 8–10, the slopes of *E vs.* pH are −68, −88, −67, and 52 mV per pH unit, respectively. Above pH 8.9, the cyclic voltammogram was drawn out with an asymmetric shape. Above pH > 10, the complex on the ITO electrode was easily desorbed from the ITO surface. Therefore, the proton-coupled electron transfer reaction of $[Ru_2(bpbbip)_2(H4L0)]^{n+}$ occurred on the immobilized ITO electrode over the pH range of 1~10. For the immobilized Ru complex, a total of eight protons can be dissociated from the immobilized Ru complex on the ITO electrode, ignoring the protons on the two anchored phosphonate groups. While the pK_a values of phosphonate head groups can be expected to fall within pK_{a1} < 2 and pK_{a2} ~ 6, we have not succeeded in the determination of all pK_a values (see Scheme 5).

Electrochromic response of the immobilized Ru complex on an ITO electrode

Spectroelectrochemical measurements of the immobilized $[Ru_2(bpbbip)_2(H4L0)](PF_6)_4$ on an ITO electrode at pH 6.5 (ionic strength = 0.1 M $NaClO_4$) were carried out under thin-layer UV conditions. Fig. 7 shows the differential spectra of the immobilized ITO electrode on the oxidative condition at +0.8 V *vs.* Ag–AgCl and the spectral response monitored at 540 nm by applying the potential pulse. The difference absorption spectrum exhibits a strong bleaching of the MLCT band at 550 nm and the π–π* transition of ligands at 364 nm and an absorption enhancement at 400 and 640 nm (Fig. 7a). When a 30 ms interval potential pulse was applied to the ITO electrode, the corresponding absorption response at 550 nm was observed even at monolayer thickness. Therefore, the immobilized Ru complex was stable for repeated oxidation and this electrode has potential for electrochromic applications. The multilayer formation of this monolayer by the combination of Zr(IV) or Cu(II) ion is also possible, which is beyond the scope of this paper.

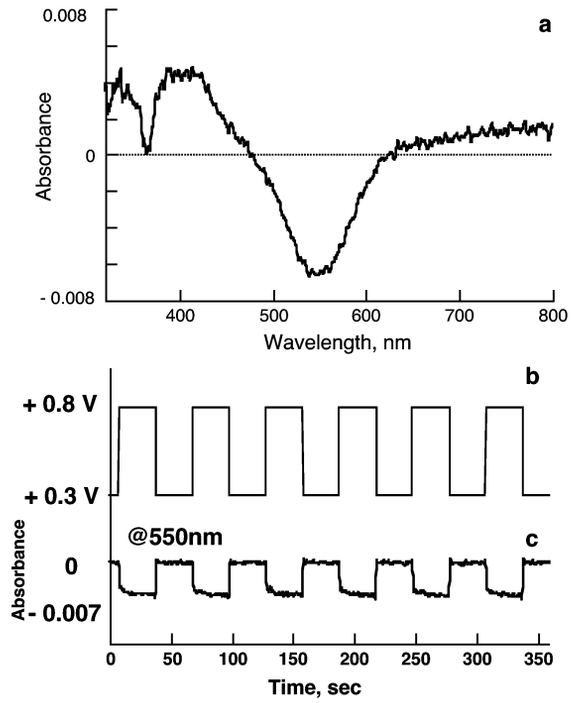

Fig. 7 (a) The differential UV absorption spectra of the immobilized Ru complex on an ITO electrode upon the oxidative condition at +0.80 V *vs.* Ag–AgCl and (b) the pulse sequence for the applied potential from +0.4 to +0.8 V and (c) the corresponding UV response of absorbance at 550 nm.

Acknowledgements

M. H. gratefully acknowledges financial support from the Institute of Science and Engineering at Chuo University, the Ministry of Education, Science, Sports and Culture for a Grant-in-Aid for Scientific Research (no. 12440188), and also support from the Promotion and Mutual Aid Corporation for Private Schools of Japan.

References

1 (*a*) C. Joachim, J. K. Gimzewski and A. Aviram, *Nature*, 2000, **408**, 541–548; (*b*) Y. Wada, M. Tsukada, M. Fujihira, K. Matsushige, T. Ogawa, M.-a. Haga and S. Tanaka, *Jpn. J. Appl. Phys.*, 2000, **39**, 3835–3849.
2 J. Jortner and M. Ratner, *Chemistry for the 21st Century "Molecular Electronics"*, Blackwell Science, Oxford, 1997.
3 R. Ziessel, *Synthesis*, 1999, 1839–1865.
4 C. Patoux, J.-P. Launay, M. Beley, S. Chodorowski-Kimmes, J.-P. Collin, S. James and J.-P. Sauvage, *J. Am. Chem. Soc.*, 1998, **120**, 3717–3725.
5 P. J. Mosher, G. P. A. Yapand and R. J. Crutchley, *Inorg. Chem.*, 2001, **40**, 1189–1195.
6 M. T. Indelli, F. Scandola, J.-P. Collin, J.-P. Sauvage and A. Sour, *Inorg. Chem.*, 1996, **35**, 303–312.
7 M. Hissler, A. El-ghayoury, A. Harriman and R. Ziessel, *Angew. Chem., Int. Ed.*, 1998, **37**, 1717–1720.
8 A. Harriman, A. Khatyr, R. Ziessel and A. C. Benniston, *Angew. Chem., Int. Ed.*, 2000, **39**, 4287–4290.
9 L. M. Vogler and K. J. Brewer, *Inorg. Chem.*, 1996, **35**, 818–24.
10 E. Sondaz, J. Jaud, J.-P. Launay and J. Bonvoisin, *Eur. J. Inorg. Chem.*, 2002, 1924–1927.
11 L. Hammarstrom, F. Barigelletti, L. Flamigni, N. Armaroli, A. Sour, J.-P. Collin and J.-P. Sauvage, *J. Am. Chem. Soc.*, 1996, **118**, 11972–11973.
12 R. Schlicke, P. Belser, L. D. Cola, E. Sabbioni and V. Balzani, *J. Am. Chem. Soc.*, 1999, **121**, 4207–4214.
13 I. M. Dixon and J.-P. Collin, *J. Porphyrins Phthalocyanines*, 2001, **5**, 600–607.
14 M.-a. Haga, M. M. Ali, H. Maegawa, K. Nozaki, A. Yoshimura and T. Ohno, *Coord. Chem. Rev.*, 1994, **132**, 99–104.
15 M.-a. Haga, T. Ano, K. Kano and S. Yamabe, *Inorg. Chem.*, 1991, **1991**, 3843.

16 M.-a. Haga, M. M. Ali, S. Koseki, K. Fujimoto, A. Yoshimura, K. Nozaki, T. Ohno, K. Nakajima and D. J. Stufkens, *Inorg. Chem.*, 1996, **35**, 3335.
17 M.-a. Haga, M. M. Ali and R. Arakawa, *Angew. Chem., Int. Ed. Engl.*, 1996, **35**, 76–78.
18 A. Credi, V. Balzani, S. J. Langford and J. F. Stoddart, *J. Am. Chem. Soc.*, 1997, **119**, 2679–2681.
19 C. P. Collier, J. O. Jeppesen, Y. Luo, J. Perkins, E. W. Wong, J. R. Heath and J. F. Stoddart, *J. Am. Chem. Soc.*, 2001, **123**, 12632–12641.
20 A. P. d. Silva, H. Q. Gunaratne and C. P. McCoy, *J. Am. Chem. Soc.*, 1997, **119**, 7891–7892.
21 C. G. Cameron and P. G. Pickup, *J. Am. Chem. Soc.*, 1999, **121**, 7710–7711.
22 C. G. Cameron, T. J. Pittmanand and P. G. Pickup, *J. Phys. Chem. B*, 2001, **105**, 8838–8844.
23 E. C. Constableand and M. D. Ward, *J. Chem. Soc., Dalton Trans.*, 1990, 1405–1409.
24 E. C. Constable and A. M. W. C. Thompson, *J. Chem. Soc., Dalton Trans.*, 1992, 3467–3475.
25 E. C. Constable, A. M. W. C. Thompson and S. Greulich, *J. Chem. Soc., Chem. Commun.*, 1993, 1444–6.
26 E. C. Constable and A. M. W. C. Thompson, *J. Chem. Soc., Dalton Trans.*, 1995, 1615–1627.
27 A. W. Addison and P. J. Burke, *J. Heterocycl. Chem.*, 1981, **18**, 803.
28 J. B. Lamture, Z. H. Zhou, A. S. Kumar and T. G. Wensel, *Inorg. Chem.*, 1995, **34**, 864–869.
29 M.-a Haga, N. Kato, H. Monjushiro, K. Wang and M. D. Hossain, *Supramol. Sci*, 1998, **5**, 337.
30 M. D. Hossain, R. Ueno and M.-a. Haga, *Inorg. Chem. Commun.*, 2000, **3**, 35–38.
31 B. Whittle, N. S. Everest, C. Howard and M. D. Ward, *Inorg. Chem.*, 1995, **34**, 2025–32.
32 T. Yutaka, M. Kurihara and H. Nishihara, *Mol. Cryst. Liq. Cryst. Sci. Technol., Sect. A*, 2000, **343**, 193–198.
33 T. Yutaka, I. Mori, M. Kurihara, J. Mizutani, K. Kubo, S. Furusho, K. Matsumura, N. Tamai and H. Nishihara, *Inorg. Chem.*, 2001, **40**, 4986–4995.
34 G. R. Newkome, T. J. Cho, C. N. Moorefield, R. Cush, P. S. Russo, L. A. Godinez, M. J. Saunders and P. Mohapatra, *Chem. Eur. J.*, 2002, **8**, 2946–2954.
35 S. Kelch and M. Rehahn, *Chem. Commun.*, 1999, 1123–1124.
36 S. W. Jones, M. R. Jordan and K. J. Brewer, *Molecular and Supramolecular Photochemistry*, Marcel Dekker, Inc., New York, 1999, vol. 4, pp. 151–183.
37 K. J. Brewer, *Comments Inorg. Chem.*, 1999, **21**, 201–224.
38 P. Ceroni, A. Credi, V. Balzani, S. Campagna, G. S. Hanan, C. R. Arana and J.-M. Lehn, *Eur. J. Inorg. Chem.*, 1999, 1409–1414.
39 C. M. Chamchoumis and P. G. Potvin, *J. Chem. Soc., Dalton Trans.*, 1999, 1373–1374.
40 V. Grosshenny, F. M. Romero and R. Ziessel, *J. Org. Chem.*, 1997, **62**, 1491–1500.
41 J.-D. Lee, L. M. Vrana, E. R. Bullockand and K. J. Brewer, *Inorg. Chem.*, 1998, **37**, 3575–3580.
42 J.-P. Collin, P. Laine, J.-P. Launay, J.-P. Sauvage and A. Sour, *J. Chem. Soc., Chem. Commun.*, 1993, 434–5.
43 F. Barigelletti, L. Flamigni, V. Balzani, J.-P. Collin, J.-P. Sauvage, A. Sour, E. C. Constable and A. M. W. C. Thompson, *J. Am. Chem. Soc.*, 1994, **116**, 7692–7699.
44 V. Grosshenny, A. H. Harriman and R. Ziessel, *Angew. Chem., Int. Ed. Engl.*, 1995, **34**, 2705–2708.
45 D. R. Baghurst and D. M. Mingos, *Microwave-Enhanced Chemsitry*, American Chemical Society, Washington, D.C., 1997, ch. 10.
46 T. E. Mallouk, H.-N. Kim, P. J. Ollivier and S. W. Keller, *Comprehensive Supramolecular Chemistry*, 1996, vol. 7, pp. 189–217.
47 A.-M. Andersson, R. Isovitsch, D. Miranda, S. Wadhwa and R. H. Schmehl, *Chem. Commun.*, 2000, 505–506.
48 L. Hammarstrom, F. Barigelletti, L. Flamigni, M. T. Indelli, N. Armaroli, G. Calogero, M. Guardigli, A. Sour, J.-P. Collin and J.-P. Sauvage, *J. Phys. Chem. A*, 1997, **101**, 9061–9069.
49 M. Maestri, N. Armaroli, V. Balzani, E. C. Constable and A. M. W. C. Thompson, *Inorg. Chem.*, 1995, **34**, 2759–2767.
50 X. Xiaoming, M.-a Haga, T. Matsumura-Inoue, Y. Ru, A. W. Addison and K. Kano, *J. Chem. Soc., Dalton Trans.*, 1993, 1993.
51 V. Balzani, A. Juris, M. Venturi, S. Campagna and S. Serroni, *Chem. Rev.*, 1996, **96**, 759–833.
52 A. Ulman, *Chem. Rev.*, 1996, **96**, 1533–1554.
53 W. J. Hehre, B. J. Deppmeier and P. E. Klunzinger, PC Spartan Pro Tutorial, Wavefunction Inc., Irvine, CA, 1999.